

Engineered Design of Mesoporous Silica Nanoparticles to Deliver Doxorubicin and P-Glycoprotein siRNA to Overcome Drug Resistance in a Cancer Cell Line

Huan Meng,^{†,‡} Monty Liong,^{‡,§} Tian Xia,^{†,‡} Zongxi Li,[‡] Zhaoxia Ji,^{||} Jeffrey I. Zink,^{‡,||} and Andre E. Nel^{†,§,||,*}

[†]Division of NanoMedicine, Department of Medicine, [‡]Department of Chemistry & Biochemistry, [§]The Southern California Particle Center, and ^{||}California NanoSystems Institute, University of California, Los Angeles, California 90095. *These authors contributed equally to this work.

owing to their unique structure and ease with which the surface can be functionalized, mesoporous silica nanoparticles (MSNP) constitute a multifunctional platform that can be used for drug^{1–4} and nucleic acid delivery.⁵ For therapeutic purposes, we prefer nanoparticles that contain a phosphonate surface coating because of the ease of particle dispersal and good biosafety index as well as the ability to adsorb cationic polyethylenimine (PEI) polymers for complexing and delivery of DNA and siRNA.⁵ Since the polymer attachment leaves the porous interior free for drug binding and delivery, it establishes the potential to achieve simultaneous drug and nucleic acid delivery.⁶ There are a number of circumstances where dual drug and siRNA delivery could achieve a synergistic therapeutic outcome. One example is the restoration of drug sensitivity in cancer cells by the knockdown of genes that are involved in the resistance to one or more chemotherapeutic agents. An example is the inducible P-glycoprotein (Pgp) gene that encodes for a gene product known as the multiple drug resistance protein 1 (MDR-1).⁷ Pgp is constitutively expressed in normal cells such as capillary endothelial cells in the blood brain barrier but also is selectively overexpressed in carcinomas of the stomach, breast, pancreas, and cervix in response to a number of chemotherapeutic agents.⁸ If overexpressed, Pgp could lead to drug resistance because MDR-1 contributes to the formation of a drug efflux pump that prevents the intracellular buildup of chemotherapeutic agents.⁹ Because Pgp overexpression is one of the major mechanisms of multiple drug resistance (MDR) in cancer

ABSTRACT Overexpression of drug efflux transporters such as P-glycoprotein (Pgp) protein is one of the major mechanisms for multiple drug resistance (MDR) in cancer cells. A new approach to overcome MDR is to use a co-delivery strategy that utilizes a siRNA to silence the expression of efflux transporter together with an appropriate anticancer drug for drug resistant cells. In this paper, we report that mesoporous silica nanoparticles (MSNP) can be functionalized to effectively deliver a chemotherapeutic agent doxorubicin (Dox) as well as Pgp siRNA to a drug-resistant cancer cell line (KB-V1 cells) to accomplish cell killing in an additive or synergistic fashion. The functionalization of the particle surface with a phosphonate group allows electrostatic binding of Dox to the porous interior, from where the drug could be released by acidification of the medium under abiotic and biotic conditions. In addition, phosphonate modification also allows exterior coating with the cationic polymer, polyethylenimine, which endows the MSNP to contemporaneously deliver Pgp siRNA. The dual delivery of Dox and siRNA in KB-V1 cells was capable of increasing the intracellular as well as intranuclear drug concentration to levels exceeding that of free Dox or the drug being delivered by MSNP in the absence of siRNA codelivery. These results demonstrate that it is possible to use the MSNP platform to effectively deliver a siRNA that knocks down gene expression of a drug exporter that can be used to improve drug sensitivity to a chemotherapeutic agent.

KEYWORDS: mesoporous silica nanoparticles · drug resistance · doxorubicin · P-glycoprotein (Pgp) · synergistic effects · siRNA delivery

cells, knockdown of Pgp gene expression by nanoparticle siRNA delivery could help to restore the intracellular drug levels to the concentrations required for induction of apoptosis and cytotoxicity. Thus, dual drug and siRNA delivery by nanoparticles can be used to overcome drug resistance in MDR cancer cells.

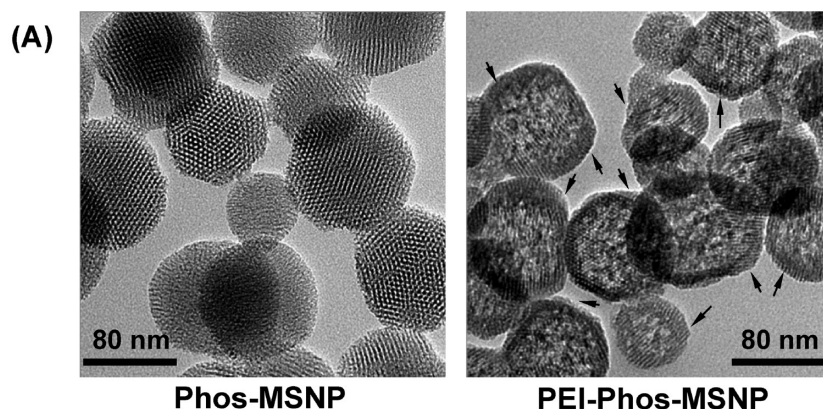
To test the utility of MSNP as a dual delivery platform, we used the drug-resistant squamous carcinoma cell line, KB-V1, to see if Pgp knockdown restores doxorubicin (Dox) sensitivity. KB-V1 cells exhibit MDR as a result of Pgp overexpression.¹⁰ To effectively engineer particles to deliver Dox as well as Pgp siRNA, it was necessary to demonstrate that particle functionalization by the attachment of negative (phosphonate)

*Address correspondence to
anel@mednet.ucla.edu.

Received for review April 5, 2010
and accepted July 06, 2010.

Published online July 14, 2010.
10.1021/nn100690m

© 2010 American Chemical Society



(B)

MSNPs Exterior	Size in H ₂ O (nm)	Size in BSA (nm)	Size in CDMEM (nm)	Zeta Potential in H ₂ O / CDMEM (mV)
PEI 1.8 kD-MSNPs	1201	360	294	+29.5/-4.6
PEI 10 kD-MSNPs	758	241	261	+34.1/-3.8
PEI 25 kD-MSNPs	1152	247	252	+31.7/-3.7

Figure 1. Physicochemical characterization of PEI-coated MSNP. (A) TEM image of phosphonate-MSNPs before and after coating with the 10 kD PEI polymer. The arrows indicate that the polymer decorates the MSNP surface but leaves the porous interior accessible to drug loading. (B) Particle size and zeta potential in pure water, after stabilization with 1 mg/mL BSA in water, or in DMEM cell culture medium, were measured. None of the size and zeta potential data are not significantly changed when the MSNP were loaded with Dox and siRNA (Supporting Information, Figure S2).

as well as positive (PEI) surface groups is functionally effective. Moreover, since PEI delivery of siRNA constructs to the cytosol requires intermediary lysosomal processing, we were also interested to determine whether this endocytic route is appropriate for Dox delivery. We demonstrate that Dox can be stably attached to the porous interior by a proton-sensitive electrostatic binding interaction that allows effective drug release from the acidifying LAMP-1-positive compartment. Pgp siRNA co-delivery increases intracellular Dox concentrations with improved cytotoxic killing. The improvement of Dox resistance provides proof-of-principal testing that MSNP can be engineered to provide contemporaneous drug and siRNA delivery by effective use of charge and the state of protonation or deprotonation at the particle surface.

RESULTS

PEI-Coated MSNP Effectively Deliver Pgp siRNA and Knock down Pgp Expression in KB-V1 Cells. We confirmed the status of KB-31 and KB-V1 cells lines as Dox-sensitive and Dox-resistant cell lines, with IC₅₀ values of 0.21 and 53.0 μg/mL, respectively (Supporting Information, Figure S1A). We also confirmed through immunoblotting analysis that the Pgp expression in KB-V1 was >1000 times that of KB-31 cells (Supporting Information, Figure S1B). To determine if Pgp overexpression in KB-V1 cells is impacted by Pgp siRNA delivery, PEI polymers in the size range 1.8–25 kD were electrostatically bound to the phosphonate-MSNPs surface. Polymer binding to our 100–120 nm size MSNP, exhibiting uniform pore sizes

of 2–2.5 nm was confirmed by transmission electron microscopy (TEM) (Figure 1A, left). The TEM image of the particles decorated with the 10 kD polymer shows that the surface coating (arrows) did not occupy the porous interior (Figure 1A, right). To optimize the particle dispersal for biological experimentation, the PEI-coated particles were further treated with 1 mg/mL BSA before transfer to the complete cell culture medium. A BSA coating significantly improves particle dispersal in water as well as salt-containing complete Dulbecco's modified eagle's medium (DMEM) (Figure 1B). While the PEI-coated particles exhibit a high positive zeta potential value in water, this value changes to slightly negative upon dispersal in complete DMEM containing FCS (Figure 1B). Note that similar analysis was also performed on the Dox loaded PEI-MSNPs samples with or without siRNA binding, and that no significant changes were found with or without cargo loading (Supporting Information, Figure S2).

To determine the optimal N/P ratios for Pgp siRNA delivery, we used agarose gel electrophoresis to evaluate the binding of various amounts of siRNA to MSNP coated with the different polymer lengths as shown in Figure 2A. This demonstrated that binding capacity increases with increasing size of PEI polymers, indicating that all siRNA was bound at a N/P ratio >16 (PEI 1.8 kD), >16 (PEI 10 kD) and >8 (PEI 25 kD). On the basis of these results, we used N/P ratios of 80, 80, and 10 for polymer lengths of 1.8, 10, or 25 kD, respectively, for siRNA knock-down experiments. It is worth mentioning that Dox trapped in the pores of MSNP does not

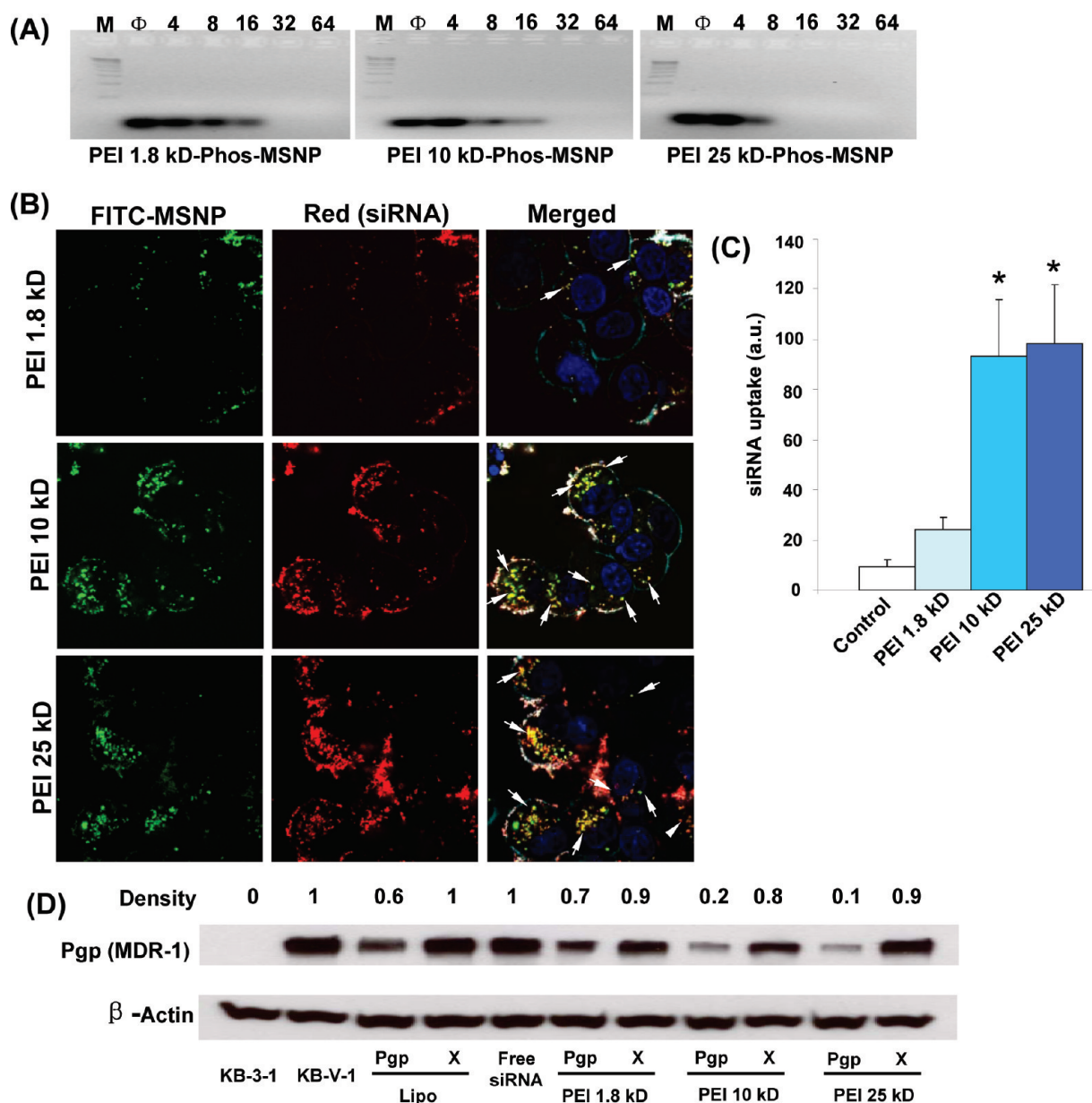


Figure 2. Effective Pgp siRNA delivery and gene knockdown in KB-V1 cells. (A) Agarose gel electrophoresis of PEI-coated MSNP to which Pgp siRNA was complexed at various nanoparticle to nucleic acid (N/P) ratios. M is molecular weight marker. The Φ lane contains Pgp siRNA only. Dox loading did not change the N/P ratio or the electrophoretic mobility. The results indicate that all siRNA was bound when the N/P ratio was >16 (PEI 1.8 kD), >16 (PEI 10 kD), and >8 (PEI 25 kD). (B) Confocal microscopy to demonstrate Texas red-labeled siRNA uptake in association with FITC-labeled PEI coated MSNP. The cell membrane and nucleus were stained by WGA 633 and Hoechst 33342, respectively. The panels on the right show merging of the images to show Pgp siRNA colocalization with FITC-MSNP. (C) Quantitative comparison of labeled Pgp siRNA uptake by measuring fluorescent intensity of Texas red in various PEI groups, using Imaging J software. Asterisks (*) indicate $p < 0.05$. (D) Detection of Pgp knockdown by siRNA-PEI-MSNP using Western blotting. Lipofectamine 2000 was used as positive control. The relevant Pgp expression was calculated by the signal intensity of the protein bands. "X" stands for cells treated by scrambled siRNA-PEI-MSNP.

influence siRNA binding to the particle surface (Supporting Information, Figure S3) and also that siRNA binding does not significantly change the zeta potential of MSNP (Supporting Information, Figure S2). Subsequent performance of confocal microscopy utilizing dual-labeled particles (Texas red-labeled siRNA adsorbed to FITC-labeled MSNP) demonstrated a high rate of cellular uptake in KB-V1 cells in accordance with polymer length (Figure 2B). Image J analysis confirmed a significant increase in siRNA uptake for particles

coated with the 10 and 25 compared to the 1.8 kD polymer (Figure 2C). The reason for this high uptake is due to the positively charged amines, which facilitates strong PEI binding to and wrapping by the surface membrane.⁵ Please notice that the Pgp siRNA (red) and FITC-MSNP (green) colocalize (yellow, merged) in the cell, demonstrating that the nucleic acid is stably attached to the PEI-coated particle surface (Figure 2B). We have previously demonstrated that nucleic acids bound to the PEI-MSNP surface are resistant to enzymatic cleavage.⁵

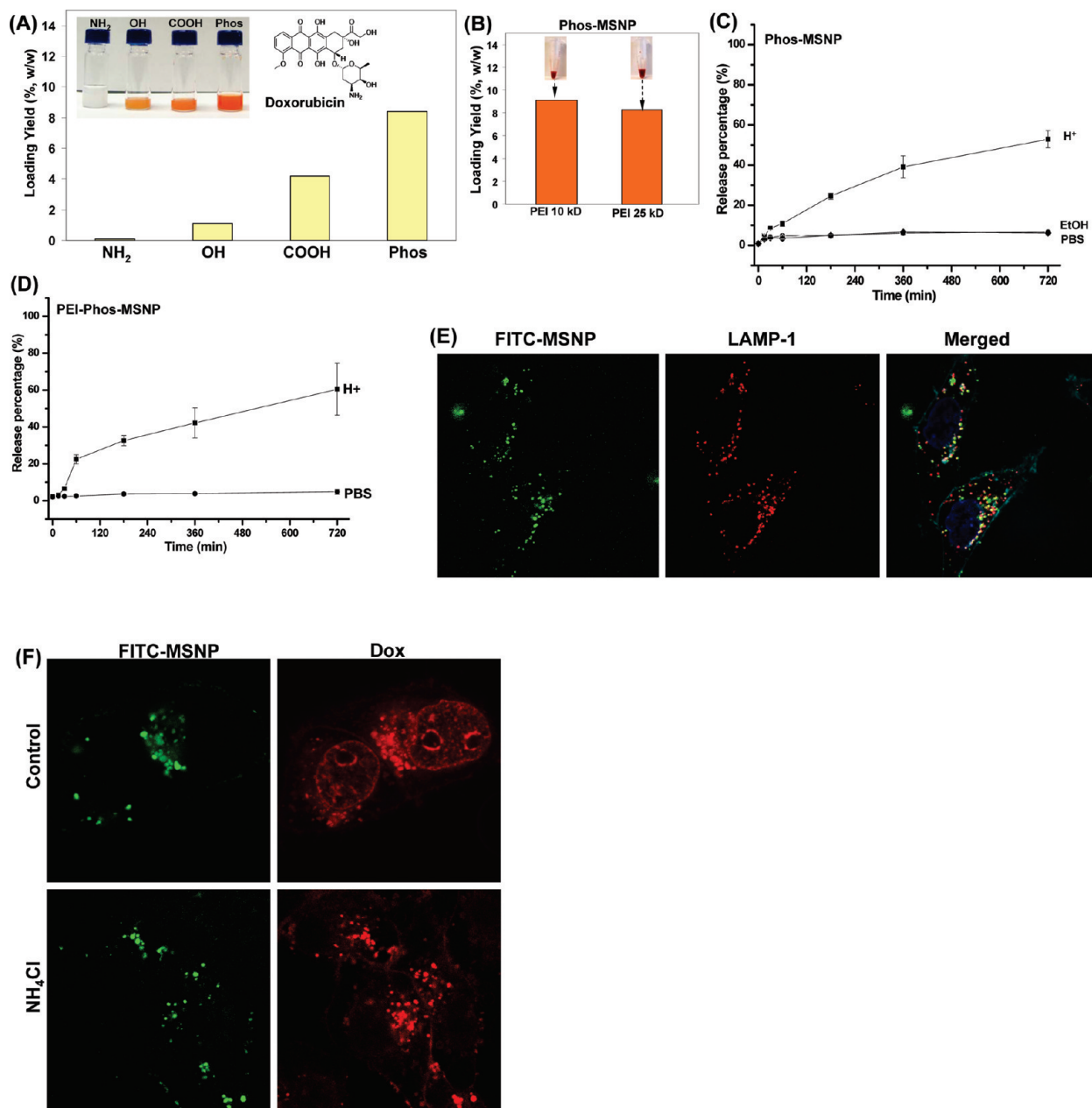


Figure 3. Phosphonate-MSNPs effectively bind Dox *via* a proton-sensitive mechanism. (A) Modeling studies using positively and negatively charged MSNP under abiotic conditions. Loading yield of Dox in MSNP with various surface modifications. Photographs of the Dox-loaded MSNP (20 mg/mL) containing various surface modifications were taken. Consistent with loading yield, the phosphonate-MSNPs were more intensively stained (red) than other particle types. (B) Loading yield measurements for PEI-coated phosphonate MSNP. The yields were similar to that of noncoated particles in panel A. (C) The time-dependent release profile of Dox from drug loaded phosphonate MSNP in phenol-red-free DMEM acidified to pH 5.0. The effect of PBS or treatment with PBS containing 10% ethanol is shown for comparison. We define I_t as the fluorescent intensity of released Dox at certain time point; I_0 as the total Dox fluorescence signal intensity that can be recovered by repeated acid washing (considered as 100% release). The release percentage equals $(I_t/I_0) \times 100$. (D) Dox release from phosphonate-MSNPs coated with the 10 kD PEI polymer under similar acidification conditions; this demonstrates that the polymer does not interfere in drug release. (E) Confocal microscopy showing FITC-labeled MSNP uptake into the LAMP-1⁺ compartment in KB-V1 cells. The yellow spots in the merged image show the colocalization. Calculation of colocalization ratio by Imaging J software indicates >55% colocalization of the green-labeled particles with the red-labeled lysosomes. (F) Confocal microscopy showing Dox release from the MSNP to the nucleus in KB-V1 cells 72 h after the introduction of the particles. The bottom panel shows that the lysosomal pH neutralizer, NH₄Cl, interferes in drug release.

To assess the efficacy of Pgp siRNA delivered by PEI-coated MSNP, Pgp expression was followed by Western blotting (Figure 2D). This demonstrated 80 or 90% reduction in MDR-1 expression in cells treated with MSNP-coated particles that contain the 10 and 25 kD polymers, respectively. This efficacy was maintained in

Dox-loaded MSNP (Supporting Information, Figure S4). Scrambled siRNA-PEI-MSNPs (marked as "X" in Figure 2D) was used as a negative control to rule out any impact by the siRNA delivery method. No Pgp knockdown was seen in the scrambled siRNA-MSNPs group. The PEI-coated particles were also more effective than the

commercially available transfection agent, Lipofectamine 2000, which is widely used in molecular biology.

An important consideration in the use of PEI is its potential cytotoxicity.⁵ In this regard, we have recently shown that polymer size plays an important role in the cytotoxicity that results from proton sequestration by unsaturated PEI amines in the lysosomal compartment.⁵ Thus, before the performance of Dox-induced cytotoxicity test, it was necessary to compare the cytotoxic potential of MSNP coated with different PEI polymer lengths as shown in the Supporting Information, Figure S5. In brief, the findings were that MSNP coated with the 25 kD polymer shows considerable toxicity in the MTS assay when the particle concentration is >25 $\mu\text{g/mL}$. By contrast, particles coated with 10 kD PEI have no toxic effects if the concentration is kept <100 $\mu\text{g/mL}$ and the exposure time is limited to ≤ 24 h (Supporting Information, Figure S5). Consequently, we used MSNP at doses <100 $\mu\text{g/mL}$ and for exposure time periods <24 h in the drug delivery studies to avoid effects on cell viability. Although no cytotoxicity was seen with the 1.8 kD PEI polymer (Supporting Information, Figure S5A), this particle is relatively ineffective for siRNA delivery and Pgp knockdown (Figure 2B,C,D).

PEI-Coated MSNP Efficiently Bind and Deliver Dox via a Proton-Sensitive Mechanism. We have recently demonstrated that MSNP are capable of loading and releasing water-insoluble drugs (paclitaxel and camptothecin) by a phase transfer mechanism that can be reversed by ethanol washing of the particles to demonstrate the role of hydrophobicity in MSNP drug entrapment.^{5,11} A key question was whether similar effective packaging of water-soluble Dox, is possible at physiological pH, where the drug ($\text{p}K_{\text{a}} = 8.2$) carries a positive charge. One conceivable approach is electrostatic attachment to the negatively charged MSNP surface. To test this possibility, Dox was loaded in MSNP decorated with OH, COOH, or phosphonate groups. These particles were also compared to positively charged particles decorated with amine groups. After washing of the drug-bound particles and quantification of Dox release by HCl, the loading capacities of OH-, COOH-, and phosphonate-MSNP were 1.2%, 4.2%, and 8.4% (w/w), respectively (Figure 3A). By contrast, amine-decorated particles showed low ($<0.1\%$, w/w) Dox binding capacity (Figure 3A). The principle of electrostatic binding to a negatively charged particle surface was also demonstrated through the use of a cationic dye, Hoechst 33342, which bound to a negative but not a positive MSNP surface (Supporting Information, Figure S6). Importantly, electrostatic binding of Dox to the phosphonate surface was not negated when the particles were also coated with 10 or 25 kD PEI polymers; these particles demonstrated an equivalent loading capacity to the uncoated phosphonate particles (Figure 3B).

Importantly, Dox could be released in a time-dependent manner from the phosphonate-MSNP or

PEI-phosphonate-MSNP surface by lowering of the solution pH (Figure 3C,D). The Dox release profile was not affected by the siRNA binding to PEI on the exterior surface of the particle (Supporting Information, Figure S7). This establishes the possibility that intracellular drug release should be possible if the particles are capable of gaining entrance to acidifying cellular compartments. To determine whether this is possible in KB-V1 cells, we studied the intracellular localization of FITC-labeled MSNP in relation to lysosomal costaining by fluorescent labeled anti-LAMP-1 antibody. Indeed, confocal microscopy confirmed $>55\%$ colocalization of the green-labeled particles with the red-labeled lysosomes (Figure 3E). Moreover, in a subsequent confocal study we demonstrated that released Dox from PEI-coated particles after entrance into the lysosome could reach the nucleus, which was brightly stained by the fluorescent drug (Figure 3F, upper panel). Please notice that some of the drug was retained in particles localized in the peri-nuclear region. This visual image changed completely when cells were treated with NH_4Cl ; most Dox remained confined to the lysosomal compartment with little or no nuclear staining (Figure 3F, lower panel). This suggests that the interference in lysosomal acidification by NH_4Cl prevents effective Dox release to KB-V1 nuclei.

Dual Delivery of Dox and Pgp siRNA Partially Restores Drug Sensitivity in KB-V1 Cells. We have already discussed the relative inefficiency of free Dox to induce KB-V1 cytotoxicity as a result of the rapid rate by which the drug was being exported by the overexpressed Pgp. Intracellular Dox concentration can be determined by measuring cellular Dox fluorescence intensity in a microplate reader (Figure 4A). The comparatively low drug uptake after treatment with free Dox was slightly improved by delivering the drug *via* the phosphonate-MSNP. While the total amount of intracellular drug increased when being delivered by particles coated with the 10 kD PEI polymer (Figure 4A), little of the drug reached the nucleus as determined by confocal imaging (Figure 4B). Interestingly, the intracellular Dox concentration increased significantly in the presence of siRNA (Figure 4A) so that there was also a significant increase in nuclear Dox staining by 72 h (Figure 4B). This contrasts with most of the Dox being confined to the endosomal compartment in cells not receiving siRNA, suggesting that although PEI-MSNP may take more Dox into to cells, any released drug is rapidly extruded from the cell before reaching the nucleus (Figure 4B). This suggests that knocking down Pgp expression (Supporting Information, Figure S4) allows a sufficient quantity of the drug being slowly released from the particle to enter the nucleus where it induces cytotoxicity. A quantitative measurement of Dox release to the nucleus through the use of Image J software confirmed a statistically significant increase of the drug in KB-V1 nuclei after delivery by siRNA-PEI-Dox-MSNP as compared to

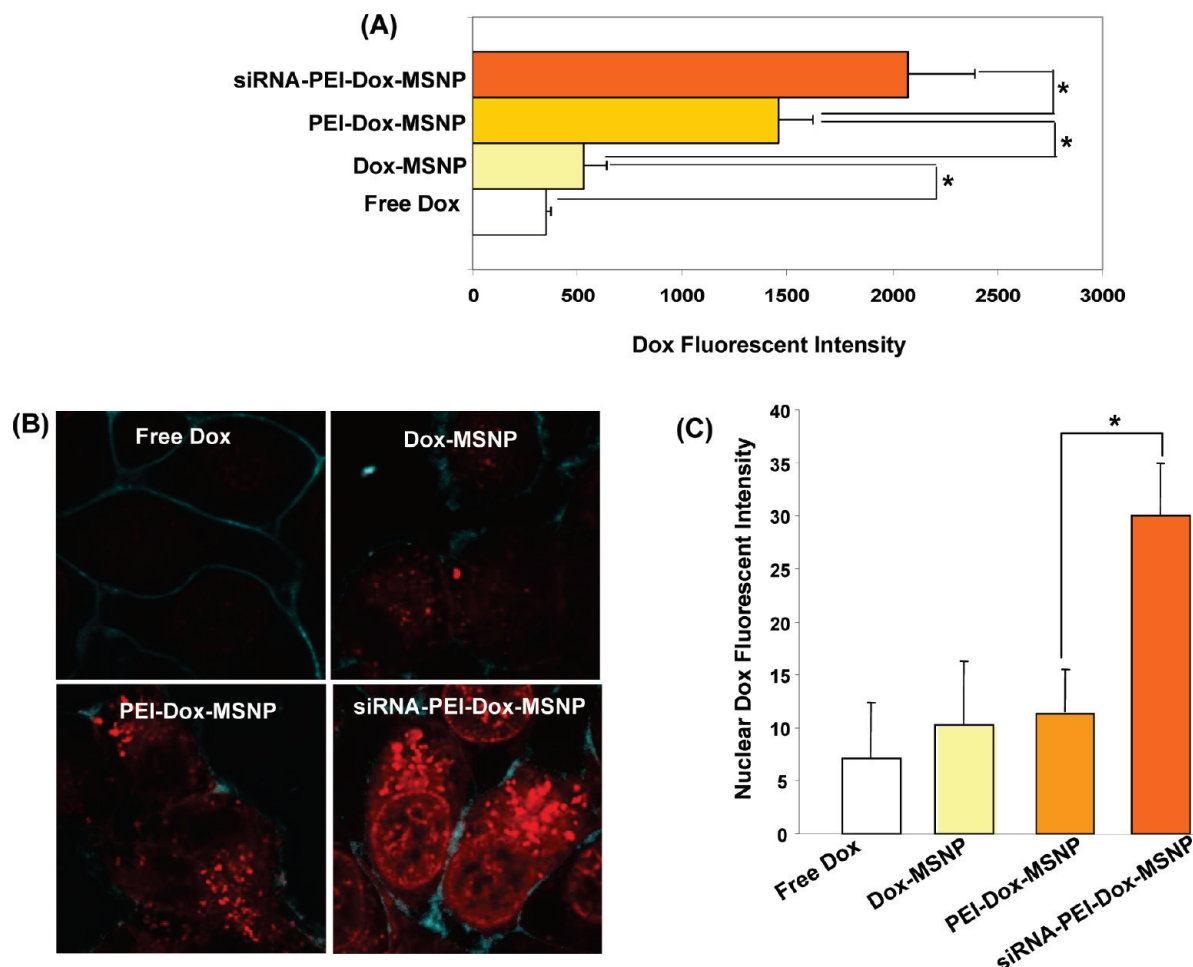


Figure 4. Simultaneous delivery of Dox and Pgp siRNA to the nucleus leads to a synergistic increase in cellular and nuclear Dox levels in KB-V1 cells. (A) Quantitative comparison of Dox levels using a fluorescent readout of cellular drug levels 72 h after introduction of treatment, using 2 $\mu\text{g}/\text{mL}$ free Dox or the equivalent amount of drug loaded into MSNP before or after PEI coating or PEI coating followed by the attachment of Pgp siRNA. (B) Confocal images showing drug uptake in KB-V1 cells that treated with 5 $\mu\text{g}/\text{mL}$ free Dox or the equivalent amount of drug loaded into various MSNPs for 72 h. Please note that while free Dox could not be maintained intracellularly, Dox delivered by MSNP (Dox-MSNP) were retained in the particles that localized in the peri-nuclear region. PEI-Dox-MSNP significantly enhanced particle uptake compared to the unmodified MSNP. However, while much of the drug remained confined to the particles, nuclear staining could be observed when Pgp siRNA was added to this platform. Thus, Pgp knockdown is likely effective at maintaining the Dox that is released from the particles long enough to allow the drug to find its way to the nucleus. The cell membrane was stained by Alexa 633-conjugated WGA (cyan color). Dox staining is in red. (C) Quantitative analysis of the nuclear fluorescence signal in KB-V1 nuclei was performed by the use of Image J software.

free Dox or Dox loaded into the particles without siRNA (Figure 4C). Dox delivered by PEI-MSNP in the presence of siRNA significantly enhances intranuclear Dox concentration when compared to free Dox or Dox delivered by MSNP or PEI-MSNP without siRNA.

To reconcile these findings with improved cell killing, we used the MTS assay to compare KB-V1 cytotoxicity under incremental Dox concentrations (Figure 5A). On the basis of the calculated IC_{50} values of the various formulations, it was possible to rank the killing efficiency as follows: siRNA-PEI-Dox-MSNP > PEI-Dox-MSNP \approx Dox-MSNP > free Dox. Moreover, the IC_{50} value of the siRNA-delivering MSNP was approximately 2.5 times lower than the IC_{50} of free Dox or other Dox-loaded particles. This suggests an additive effect between the drug and the siRNA that are being delivered by MSNP. Although it was not possible to restore drug

sensitivity to the level seen in KB-31 cells, we could clearly observe a much higher percentage of apoptotic KB-V1 cells after treatment with Dox-loaded MSNP that codeliver siRNA as compared to free Dox or Dox delivered by non-siRNA delivering particles (Figure 5B). We confirmed the flow cytometry data through the use of another apoptosis assay using TUNEL staining (Supporting Information, Figure S8), which showed an identical trend. Failure to fully restore drug sensitivity could be due to extremely high levels of Pgp expression and/or additional drug resistant pathways in KB-V1 that were not targeted in the current research. Because of the duration of time it takes for the siRNA to exert its effect, we also analyzed cell viability after longer treatment periods (e.g., 96 h) but did not observe any improvement in cytotoxicity (Supporting Information Figure S9). In addition, we also treated the KB-V1 cells by coadminis-

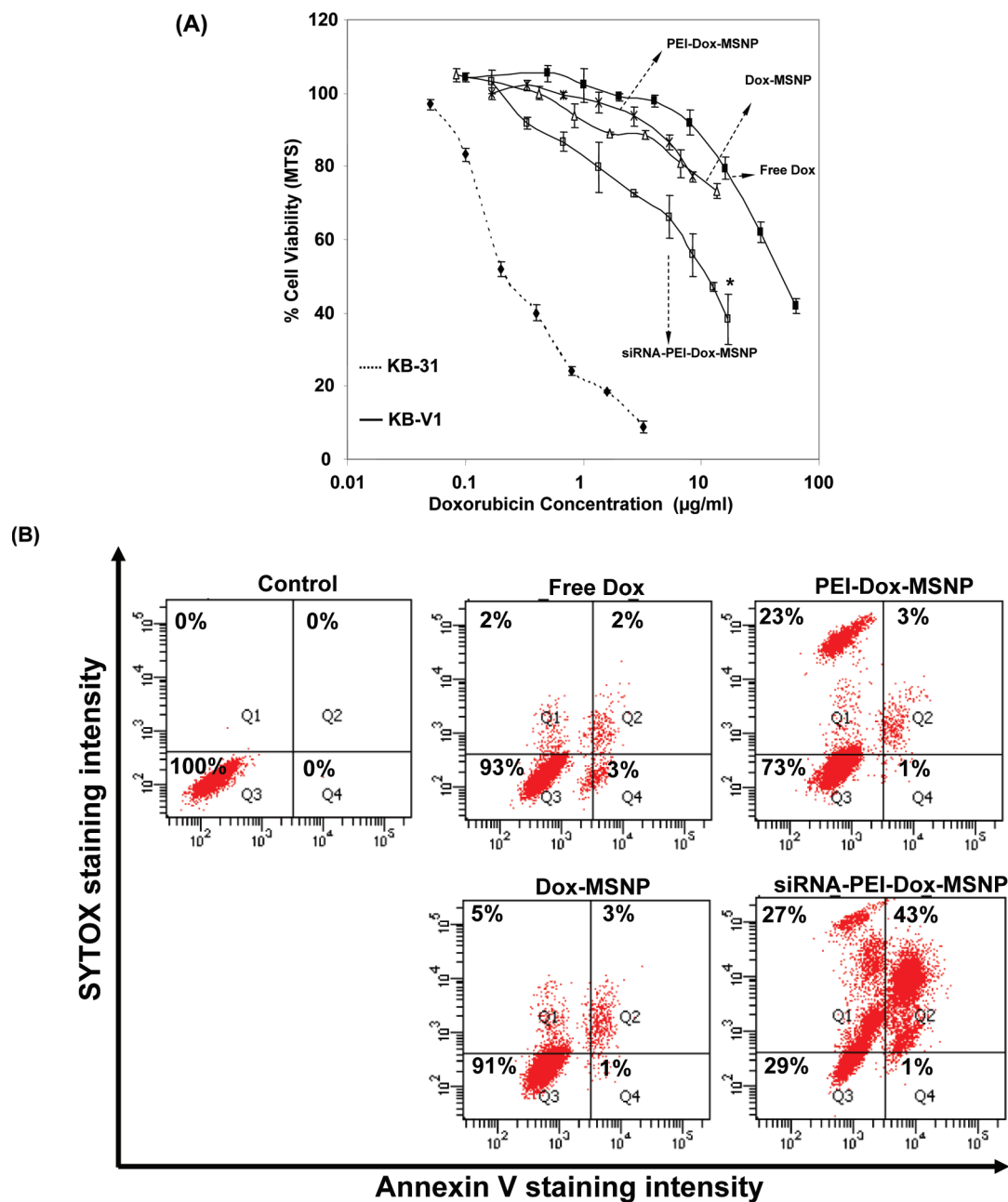


Figure 5. Comparison of the cytotoxic effects of different delivery modalities of Dox in KB-V1 cells. (A) MTS cell viability assay showing that MSNP delivery of Dox concomitant with Pgp siRNA is capable of improving the induction of cytotoxicity by free Dox or Dox delivered by PEI-coated MSNP not attached to siRNA. The broken line is the cell killing curve of free Dox in parental cell line (KB-31, Dox sensitive). (B) Annexin V-SYTOX staining showing enhanced apoptosis and cell death by siRNA-PEI-Dox compared to the other Dox modalities mentioned in panel A. The flow cytometry data were further confirmed by TUNEL staining assay (Supporting Information, Figure S8).

tration of Dox and Tariquidar, which is a potent and effective Pgp inhibitor in human clinical trial, to see if we can restore KB-V1 sensitivity to that seen in KB-31 cells. While this combination significantly improves cell killing capability in KB-V1 cells, it is incapable of completely restoring Dox sensitivity to the level seen in KB-31 cells (Supporting Information, Figure S10).

DISCUSSION

Here we show that MSNP can be functionalized to deliver a chemotherapeutic agent as well as Pgp siRNA

to a drug-resistant cancer cell line. The functionalization of the particle surface with a phosphonate group allows electrostatic binding of Dox to the porous interior, from where the drug could be released by acidification of the medium under abiotic and biotic conditions. In addition, phosphonate modification also allows exterior coating with the cationic polymer, PEI, which endows the MSNP with the ability to contemporaneously bind and deliver Pgp siRNA. The dual delivery of Dox and siRNA in KB-V1 cells was capable of increasing the intracellular as well as intranuclear drug concentra-

tion to levels exceeding that of free Dox or the drug being delivered by MSNP without siRNA codelivery. This reflects the ability of the siRNA to effectively knock down Pgp expression, therefore interfering in drug efflux as one of the resistance mechanisms in KB-V1 cells. Unlike hydrophobic cargo (Supporting Information, Figure S11), Dox can be released from the lysosome by a proton-sensitive mechanism. While clearly effective at improving cytotoxic killing through its dual delivery capabilities, siRNA-PEI-MSNP could not restore Dox sensitivity in KB-V1 to the level seen in drug-sensitive KB-31 cells. This is likely due to the extremely high levels of Pgp expression, as confirmed in Supporting Information, Figure S1.

Two of the major problems in cancer chemotherapy are toxic side effects as well as development of MDR in cancer cells. Nanoparticle drug delivery is capable of overcoming both problems through tumor cell targeting as well as the capability to overcome drug resistance.^{9,12} MDR can basically be divided into two distinct categories, namely pump and nonpump resistance.^{9,13} Pump resistance refers to the inducible formation of membrane-bound channels or pores that actively expel a series of structural and functional distinct chemotherapeutic agents from the cell. Drug efflux significantly decreases the intracellular concentration that limits their cytotoxic potential. The key proteins involved in pump resistance are Pgp and MRP-1, while the major mechanism in nonpump resistance is activation of cellular antiapoptotic defense pathways, including drug-induced expression of Bcl-2 protein.¹³ Moreover, the pump and nonpump resistance mechanisms could be mutually interactive.⁹ Given this background, a number of nanomaterial design strategies can be used to overcome drug resistance.

(i) The first strategy is codelivery of the chemotherapeutic drug with a pharmaceutical agent that interferes in pump activity or in nonpump pathways. One example is the use of verapamil as a Pgp inhibitor that has been combined with Dox, aimed at reducing cardiotoxicity of Dox as well as overcoming Pgp-mediated MDR.¹⁴ In Dox-resistant K562 leukemia cells, a liposomal Dox-verapamil complex doubled the cytotoxicity index ($IC_{50} = 11.4 \mu\text{M}$) of free Dox ($IC_{50} = 23.4 \mu\text{M}$).¹⁴ Another example is using a polymeric nanoparticle formulation of poly(ethyleneoxide)-poly(epsilon-caprolactone) to coadminister ceramide that is capable of lowering the apoptotic threshold to paclitaxel, thereby enhancing paclitaxel-induced cytotoxicity in a MDR human ovarian cancer cell line.¹⁵

(ii) A second strategy is to use nanoparticles to deliver the chemotherapeutic and siRNA that interfere in key protein expression in pump-dependent or independent drug resistance pathways. There are reports demonstrating that compared to the free drug, dual delivery with a nucleic acid is capable of enhancing the efficacy

in a synergistic fashion.^{16,17} Chen *et al.* showed that MSNP served as a drug delivery vehicle to deliver Dox and Bcl-2 siRNA that can effectively silence the Bcl-2 mRNA and significantly suppress the nonpump resistance, and therefore result in the enhanced cell killing capability of Dox in multidrug resistant A2780/AD human ovarian cancer cells.¹⁶ Another example is paclitaxel that was delivered by poly(D,L-lactide-co-glycolide) nanoparticles along with Pgp siRNA to the MDR murine mammary cancer cell line, JC. The dual delivery system showed significantly higher cytotoxicity *in vitro* and significantly greater inhibition of tumor growth *in vivo* than nanoparticles loaded with paclitaxel alone.¹⁷

(iii) The third strategy is to deliver the drug together with a combination of siRNAs that interfere in both pump (*e.g.*, Pgp) and nonpump (*e.g.*, Bcl-2) mechanisms. Such an approach may be necessitated by the coexistence of pump and nonpump resistance mechanisms.^{9,13} In this regard, it has been demonstrated that the increase in intracellular drug concentration as a result of the suppression of drug efflux pumps leads to almost proportional activation of antiapoptotic cellular defense.^{7,9} As one example, a cationic liposome carrier system was developed to deliver Dox contemporaneously with two species of siRNA targeting MRP-1 as well as Bcl-2.¹³ This triple components (Dox, MRP-1 siRNA, and Bcl-2 siRNA) delivery system demonstrated enhanced Dox cytotoxicity in human MDR H69AR lung cancer cells which showed >100 fold enhancement in cytotoxicity.¹³ Similar attempts in our own experiments in KB-V1 cells where we combined Bcl-2 with Pgp siRNA and Dox did not improve the cytotoxicity or IC_{50} significantly (not shown).

This paper demonstrates how MSNP can be engineered to effectively deliver a drug together with siRNA. Before we discuss what we learned from KB-V1 cells, it is worthwhile summarizing the key features of our interior and exterior design modifications. First, because Dox ($pK_a = 8.2$) is positively charged at physiological pH, we used a number of surface charge modifications to demonstrate the utility of using electrostatic charge to bind and deliver Dox from the MSNP surface (Figures 3A and 4B). These studies demonstrated that Dox and the cationic dye, Hoechst 33342 ($pK_a = 11.9$), are capable of binding to negatively charged surfaces from where both agents could be released by dropping the environmental pH (Figure 3C–F). Thus, when the MSNP are suspended in buffered cell culture medium (pH = 7.4), the attached phosphonate ($pK_a = 2$) and carboxylate ($pK_a = 5$) groups are deprotonated and assume a negative charge, whereas unmodified OH-MSNP ($pK_a = 7$) is near its isoelectric point and therefore not quite as effective for electrostatic binding (Figure 3A). By contrast, the amine groups ($pK_a \approx 9$) are protonated at physiological pH and exhibit a positive charge that prevents electrostatic binding of the same agents.^{18,19} From a therapeutic perspective, we focused on phosphonate-

MSNP due to good particle dispersibility and biocompatibility. The ability to release Dox from the interior surface by proton interference allowed us to achieve Dox delivery inside the cell in an acidifying compartment (Figure 3F, upper panel). The role of the lysosomal proton pump is supported by the finding that NH_4Cl interferes in Dox release to the nucleus (Figure 3F, lower panel). Phosphonate attachment also facilitates the binding of cationic PEI to the particle exterior (Figure 1A, right panel). This binding interaction is sufficiently strong to allow the polymer and attached siRNA to stay on the particle surface until entry into the lysosomal compartment. PEI may play a role in firm cellular attachment and selection of the initial endosomal compartment. Importantly, the polymer is attached to the particle surface to leave the pores accessible to Dox binding (Figure 3B).

It is important to briefly mention the importance of selecting the correct PEI polymer size to prevent particle toxicity.^{5,20,21} It is well-known that PEI exerts cytotoxic effects when used by itself or attached to the nanoparticle surface as a polyplexing agent.⁵ In this regard, we have recently demonstrated that the 25 kD PEI polymer as well as high doses of the 10 kD polymer can render the MSNP toxic as a result of the proton sponge effect in the lysosome.⁵ For these reasons, it was necessary to limit the particle dose and exposure time to within safe limits to conduct Dox and siRNA delivery with PEI 10 kD polymer (Supporting Information, Figure S5). Curiously and somewhat paradoxically, siRNA delivery to the cytosol is also dependent on the proton sponge effect of the PEI-coated particle and in this case, the lysosome appears to be a key organelle in the dual drug delivery paradigm.

The above design features extend the utility of MSNP as a drug delivery platform for chemotherapeutic agents. In addition to being able to deliver hydrophobic drugs such as camptothecin and paclitaxel, we show that it is also possible to deliver water-soluble drugs by a packaging and release mechanism that is quite different from the phase transition principle that is involved in hydrophobic drug delivery (see Supporting Information, Figure S11). While it is not possible to release hydrophobic drugs through an acidification mechanism, camptothecin can be extracted from phosphonate-MSNP pores by ethanol treatment (Supporting Information, Figure S11). The release characteristics of Dox are exactly opposite, namely a release response to protons but not ethanol (Figure 3C,D). Taken

together, these results demonstrate the dynamic features of MSNP for obtaining optimal drug packaging and delivery.

Our study demonstrates the feasibility of the MSNP platform to improve the cytotoxicity of Dox by co-delivery of Pgp siRNA as proof-of-principle. Downregulation of Pgp expression allowed the intranuclear Dox levels to increase above the threshold required for inducing apoptosis and cell death. However, since the KB-V1 cell line expresses a very high Pgp level that may go beyond the clinically relevant expression level, it may not be possible to restore drug sensitivity to the level seen in KB-31. It is reasonable to expect that the MSNP delivery platform will be more effective in a lesser Pgp expressing cell type. In addition, we also learned from the study that the MDR phenotype is quite complex and often involves a combination of drug resistance mechanisms such as increased efflux, blocked apoptosis, decreased drug influx, increased drug metabolism, and increased DNA repair.^{7,9} Preliminary research has revealed that 36 genes were either up- or down-regulated in KB-V1 cells compared to the number in KB-31 cells. These genes can be categorized into several groups, including oxidative stress regulation (HBB, IDH), drug metabolism (HMGCS1, ACAT1), signal transduction (CGA, SGK), tumor suppression (PTEN), *etc.*²² It is possible that these gene products could contribute to MDR besides Pgp overexpression. What those additional mechanisms encompass is still uncertain but apparently does not involve Bcl-2, as inclusion of Bcl-2 with Pgp siRNA did not significantly improve cell killing. The understanding of the above-mentioned MDR mechanisms may provide us new opportunities to develop more therapeutic components or combinations to achieve better therapeutic effects.

CONCLUSION

MSNP can be functionalized to act as a dual delivery vehicle for Dox as well as Pgp siRNA in a drug-resistant cancer cell line. To improve the drug sensitivity of KB-V1 cells, we used phosphonate attachment to deliver the drug as well as the siRNA *via* a lysosomal processing pathway. This dual delivery system increased the intracellular Dox levels to the extent that it improves cytotoxic killing in this KB-V1MDR cell line. This strategy could be an effective new approach for the treatment of cancers that develop multiple drug resistance.

MATERIALS AND METHODS

Materials. Tetraethylorthosilicate (TEOS, 98%), cetyltrimethylammonium bromide (CTAB, 95%), fluorescein isothiocyanate (FITC, 90%), doxorubicin hydrochloride (Dox, >98%), camptothecin (CPT, 95%), vinblastine, polyethylenimine (PEI, branched, MW 25 kD), bafilomycin A ($\geq 95\%$), ammonium chloride, β -actin

antibody, and bovine serum albumin (BSA) were from Sigma (St. Louis, MO). Polyethylenimine (branched, MW 1.8 and 10 kD) was purchased from Alfa Aesar. 3-Trihydroxysilylpropyl methylphosphonate, cyanoethyltriethoxysilane, and aminopropyltriethoxysilane were purchased from Gelest. Dulbecco's modified eagle's medium (DMEM), penicillin/streptomycin, and

L-glutamine were purchased from Invitrogen (Carlsbad, CA). Fetal calf serum (FCS) was from Atlanta Biologicals, Inc. (Lawrenceville, GA). LAMP-1 antibody was obtained from Abcam (Cambridge, MA). siRNA for Pgp knockdown was purchased from IDT Technologies (Coralville, IA). Tariquidar (>97%) was purchased from MedKoo Biosciences, Inc. For all experiments and analyses, water was deionized and filtered with a 0.45 μm pore size polycarbonate syringe filter (Millipore, Billerica, MA). All chemicals were reagent grade and used without further purification or modification.

Particle Synthesis, PEI Coating, and Interior Surface Functionalization. The MSNP were synthesized according to our previously published sol-gel procedure.^{5,11} Briefly, for the synthesis of unmodified MSNP (OH-MSNP), 100 mg of CTAB was dissolved in a solution of 48 mL of water and 0.35 mL of sodium hydroxide (2 M) and heated to 80 °C. A 0.5 mL portion of TEOS was added into the aqueous solution containing CTAB surfactants. For the phosphonate modification, 3-trihydroxysilylpropyl methylphosphonate was added to the mixture 15 min after the addition of TEOS. The CTAB surfactants were then removed from the pores by heating the particles in acidic ethanol. To perform PEI coating, 5 mg of phosphonate-modified MSNP were dispersed in a solution containing 2.5 mg PEI (1.8, 10, 25 kD) in 1 mL of absolute ethanol. After sonication and stirring for 30 min the PEI-coated particles were washed with PBS. The amount of polymer coated onto the particle surface was approximately 5 wt %.

Because Dox is positively charged under physiological pH, it was necessary to demonstrate that phosphonate or other anionic surface groups are effective for drug binding, including binding in particles that have been coated with PEI. To demonstrate this principle, we decorated particle surfaces with carboxylate (COOH) and amine groups in addition to phosphonate and silanol (OH groups). The surface functionalization was achieved by mixing organoalkoxysilanes (made up in ethanol) with TEOS before adding the mixture into the CTAB solution.²³ For carboxylate modification, 50 μL of cyanoethyltriethoxysilane was mixed with 500 μL of ethanol and 500 μL of TEOS, then added into the surfactant solution. After the surfactant removal process, the particles were further heated in a solution of 50% sulfuric acid to hydrolyze the cyanide groups into carboxylic groups. For amine modification, 50 μL of aminopropyltriethoxysilane was first mixed with 500 μL ethanol and 500 μL TEOS, and then this mixture was added to the surfactant solution. After 2 h, the solution was cooled to room temperature and the materials were washed with methanol before the surfactant removal process was performed.

Physicochemical Characterization of MSNP. PEI-coated phosphonate MSNP were characterized for size, zeta potential, and shape. The shape and porous structure were characterized using transmission electron microscopy (CM 120, Philips Electron Optics, Eindhoven, The Netherlands). Microfilms for TEM imaging were made by placing a drop of the respective MSNP suspensions onto a 200-mesh copper TEM grid (Ted Pella, Inc., Redding, CA) and then drying at room-temperature overnight. A minimum of five images for each sample was captured, and representative images were included in Figure 1A. Particle size and zeta potential in pure water, after stabilization with 1 mg/mL BSA in water, or in cell culture medium, were measured by ZetaSizer Nano (Malvern Instruments Ltd., Worcestershire, UK). All the measurements were performed in 40 $\mu\text{g}/\text{mL}$ MSNP suspensions in filtered water or filtered complete cell culture media at pH 7.4. The analysis was also studied on Dox-loaded particles. Similar analysis was also performed on cargo (Dox and siRNA)-loaded PEI-MSNP samples.

PEI-MSNP Coating with Pgp siRNA and Use of Agarose Gel Electrophoresis to Determine N/P Ratios. An agarose gel retardation assay was used to determine the siRNA binding to PEI-MSNP. A 0.1 μg portion of siRNA was mixed with 0.4–6.4 μg of PEI-MSNP in aqueous solution to obtain particle/nucleic acid (N/P) ratios of 4–64; 10 μL of the polyplex solution was mixed with 2 μL of 6 \times loading buffer and electrophoresed in a 1.5% agarose gel containing 0.5 $\mu\text{g}/\text{mL}$ ethidium bromide (EB) at 100 V for 30 min in Tris-boric acid (TBE) running buffer (pH = 8). Nucleic acid bands were detected by UV light (254 nm), and the photographs were captured in a Bio-Rad imaging system (Hercules, CA). The results

were used to calculate the threshold N/P ratios for subsequent experiments. The threshold is defined as the lowest N/P ratio value that prevents free siRNA from entering the gel. To determine the influence of Dox loading, the gel electrophoresis assay was also performed.

Cell Culture. All cell cultures were maintained in 25 cm^2 or 75 cm^2 cell culture flasks in which the cells were passaged at 70–80% confluency every 2–4 days. The drug-sensitive KB-31 line was cultured in Dulbecco's modified eagle medium (DMEM) (Carlsbad, CA) containing 10% fetal calf serum (FCS), 100 U/mL penicillin, 100 $\mu\text{g}/\text{mL}$ streptomycin, and 2 mM L-glutamine (complete DMEM medium). The MDR cell line, KB-V1 (kindly provided by Dr. Michael M. Gottesman from National Cancer Institute, NIH, Bethesda, Maryland), was maintained in 1 $\mu\text{g}/\text{mL}$ of vinblastine (made up from 10 mg/mL stock in DMSO) in complete DMEM.¹⁰ While the doubling time of the parental line was approximately 14–18 h, the resistant cell line doubled every 25–30 h.

Assessment of Cellular Uptake of Dual Fluorescent Labeled siRNA-PEI-MSNP by Confocal Microscopy. A 200 μg portion of FITC-labeled PEI-coated MSNP was incubated with 2.5 μg of Texas red-labeled Pgp siRNA for 30 min to yield a N/P ratio of 80. Cellular uptake of MSNP was performed by adding 20 $\mu\text{g}/\text{mL}$ of the dual-labeled particles to 8-well chamber slides. Each well contained 5×10^4 cells in 0.4 mL of culture medium. Cell membranes were costained with 5 $\mu\text{g}/\text{mL}$ Alexa Fluor 633-conjugated wheat germ agglutinin (WGA) in PBS for 30 min. Slides were mounted with Hoechst 33342 and visualized under a confocal microscope (Leica Confocal 1P/FCS) in the UCLA/CNSI Advanced Light Microscopy/Spectroscopy Shared Facility. High magnification images were obtained with the 100 \times objective. The signal intensity of the red channel, reflecting siRNA abundance, was calculated by Image J software (version 1.37c, NIH).

siRNA-PEI-MSNP Exposure and Assessment of PGP Expression. Pgp siRNA-PEI-MSNP complexes were freshly prepared as described above. The siRNA duplex consists of 5'-r(CGGAAGGCCUAAUGCCGAA) dTdT (sense) and 5'-r(UUCGGCAUUGGCCUCCG) dTdT (antisense) strands. First, 5 μL of 250 ng/ μL Pgp siRNA or scrambled siRNA was added to 100 μg of PEI 1.8 kD-MSNP (N/P ratio = 80), 100 μg of PEI 10 kD-MSNP (N/P ratio = 80), or 12.5 μg of PEI 25 kD-MSNP (N/P ratio = 10), in 5 μL of aqueous solution. After incubation at room temperature for 30 min, the complexes were stabilized by 1 mg/mL BSA and then transferred into 1 mL of complete DMEM. KB-V1 cells were plated at 2×10^5 cells per well, then exposed to the complexes for 16 h. After exposure, the medium was replaced with fresh DMEM containing 10% FCS and cultured for a further 56 h. Cells then were harvested for immunoblotting as outlined in the Supporting Information, section S1. A commercially available cationic liposomal transfection agent (Lipofectamine 2000) was used as a positive control. Protein abundance was quantified by densitometric scanning using a laser Personal Densitometer SI and Image Quant software (Amersham Biosciences).

Optimizing Dox Loading and Release via a Proton-Sensitive Mechanism *In Vitro*. On the basis of its cationic charge at pH 7.4, we wanted to determine whether Dox ($pK_a = 8.2$) would bind to the negatively charged porous interior, including binding under circumstances where the exterior surface was occupied by PEI. A 10 mg portion of MSNP functionalized by OH, COOH, or phosphonate attachments was mixed with 1 mg of Dox in 0.25 mL of water for 12 h. As control, we used positively charged amine-MSNP. Subsequently, the particles were collected by centrifugation and washed with water. To corroborate the electrostatic binding hypothesis, we also used the cationic fluorescent dye, Hoechst 33342 ($pK_a = 11.9$) as model cargo in the same particles. This procedure was repeated in phosphonate MSNP that were coated with 10 and 25 kD PEI polymers. To compare the loading yields of the above particles, 1 mg of Dox-loaded MSNP pellet was resuspended and sonicated in 1 mL of a heated HCl solution (pH = 5.0) for 15 min. After centrifugation, another 1 mL of fresh HCl aqueous solution was added. All the supernatants were combined until the MSNP became colorless. At this point the pH was readjusted to 7.0 by 1 M NaOH and the fluorescence spectrum of Dox was measured at excitation and emission wavelength of 485/550 nm in a microplate reader (SpectraMax M5Microplate

Reader, Molecular Device, USA). The procedure was also repeated to determine Dox loading in MSNP coated with 10 and 25 kD PEI polymers.

We also assessed the effects of acidification and ethanol extraction of Dox-loaded phosphonate MSNP; 1 mg of Dox-loaded MSNP was suspended into 3 mL of phenol red-free DMEM medium acidified to pH 5.0 or replenished with 10% (v/v) ethanol at 37 °C. The supernatants were collected at various time points and cleared by centrifugation for measurement of Dox fluorescence. Similar experiments were carried out in siRNA bound phosphonate-MSNP coated with PEI polymers. To see if the release profile would be influenced by siRNA binding, we also studied release after 12 h using siRNA-PEI-Dox-MSNP.

Confocal Microscopy to Determine MSNP Lodging in an Acidifying Cellular Compartment, Including the Effects of Inhibiting Lysosomal Acidification on Dox Release. KB-V1 cells grown on chamber slides were fixed, permeabilized, and labeled with our standard immunocytochemistry protocol.⁵ LAMP-1 staining was performed by using a 1:500 dilution of mouse-antihuman mAb (H4A3, Abcam, USA) for 16 h at 4 °C. This was followed by a 1:500 diluted TRITC-conjugated goat-antimouse secondary antibody (Santa Cruz, USA) for 1 h at room temperature. Cell membranes and nuclei were stained with WGA 633 and Hoechst 33342, respectively. Slides were visualized under a confocal microscope (Leica Confocal 1P/FCS). Since the Dox release is a proton-sensitive process, the effect of neutralizing the lysosomal pH with NH₄Cl was also investigated in KB-31 cells. These cells were initially treated with 40 µg/mL FITC-labeled MSNP that were simultaneously coated with the 10 kD PEI polymer with or without the addition of 20 mM NH₄Cl. All the images of the particles and fluorescent Dox release were captured by the same confocal microscopy applying the same parameter setting over a 72 h time period.

Determination of Intracellular Dox Concentration. Dox uptake in KB-V1 cells was quantitatively evaluated in a microplate reader at 72 h; 5 × 10⁴ cells were placed into a 96-wells plate and treated with 2 µg/mL free Dox or the equivalent amount of drug loaded into MSNP before or after PEI coating, with or without attachment of Pgp siRNA. Following the washing of the cells in cold PBS, the intracellular Dox fluorescence was detected at excitation and emission wavelength of 485/550 nm in a microplate reader (SpectraMax M5Microplate Reader, Molecular Device, USA). Moreover, we also captured confocal images at the end of experiment. Image J software (version 1.37c, NIH) was used to analyze the nuclear fluorescence.

Assessment of Cytotoxicity and Apoptosis in KB-V1 Cells Treated with Dox-Loaded Particles in the Absence and Presence of Pgp siRNA. To measure cytotoxicity of the different Dox formulations, KB-V1 cells were treated with free Dox, Dox-MSNP, PEI-Dox-MSNP, and siRNA-PEI-Dox-MSNP, respectively. For the latter two particle types, incubation time was for 16 h before replenishment of the old medium with fresh complete DMEM and performance of a MTS assay at 72 h. On the basis of the absorption readout at 490 nm, the IC₅₀ of free and Dox-loaded MSNP were calculated. We also assessed the induction of apoptosis at 72 h through the use of Annexin V-SYTOX Blue. Briefly, 5 × 10⁵ cells were harvested and stained by FITC-Annexin V- SYTOX Blue working solution (Annexin V, Trevigen; SYTOX Blue, Invitrogen) at room temperature for 15 min. The cells were washed in binding buffer before performance of flow cytometry (Becton Dickinson, Mountain View, CA). Data analysis was performed by BD CellQuest. To confirm the flow data in which there may be a minor overlap of Dox with FITC-Annexin V, a TUNEL detection kit was used according to the manufacturer's instructions to confirm the induction of apoptosis. Briefly, 72 h following treatment with free Dox or Dox-loaded particles, cells were washed, fixed, and permeabilized before TUNEL staining. The number of TUNEL-positive cells was assessed under a fluorescent microscope (200×). At least 3 fields were counted by the same investigator to calculate the percentage of TUNEL positive cells.

Statistical Analysis. Data represent the mean ± standard deviation for duplicate or triplicate measurements in each experiment, which was repeated at least three times. Differences between the mean values were analyzed by two-sided Student's *t* test or one way ANOVA, and results were considered statistically significant at *p* < 0.05.

Acknowledgment. This study was funded by the U.S. Public Health Service Grants, RO1 CA133697, RO1 ES016746 and RC2 ES018766. Support for the safety assessment of MSNP was also provided the National Science Foundation and the Environmental Protection Agency under Cooperative Agreement Number EF 0830117. The work was also supported by the NSF USDOD HDTRA 1-08-1-0041 grants. Any opinions, findings, conclusions or recommendations expressed herein are those of the author(s) and do not necessarily reflect the views of the National Science Foundation or the Environmental Protection Agency.

Supporting Information Available: Additional figures, results, and calculations. This material is available free of charge via the Internet at <http://pubs.acs.org>.

REFERENCES AND NOTES

- Lu, J.; Choi, E.; Tamanoi, F.; Zink, J. I. Light-Activated Nanoimpeller-Controlled Drug Release in Cancer Cells. *Small* **2008**, *4*, 421–426.
- Coti, K. K.; Belowich, M. E.; Liong, M.; Ambrogio, M. W.; Lau, Y. A.; Khatib, H. A.; Zink, J. I.; Khashab, N. M.; Stoddart, J. F. Mechanised Nanoparticles For Drug Delivery. *Nanoscale* **2009**, *1*, 16–39.
- Slowing, I. I.; Vivero-Escoto, J. L.; Wu, C.-W.; Lin, V. S. Y. Mesoporous Silica Nanoparticles as Controlled Release Drug Delivery and Gene Transfection Carriers. *Adv. Drug Delivery Rev.* **2008**, *60*, 1278–1288.
- Liong, M.; Lu, J.; Kovochich, M.; Xia, T.; Ruehm, S. G.; Nel, A. E.; Tamanoi, F.; Zink, J. I. Multifunctional Inorganic Nanoparticles for Imaging, Targeting, and Drug Delivery. *ACS Nano* **2008**, *2*, 889–896.
- Xia, T.; Kovochich, M.; Liong, M.; Meng, H.; Kabehie, S.; George, S.; Zink, J. I.; Nel, A. E. Polyethyleneimine Coating Enhances the Cellular Uptake of Mesoporous Silica Nanoparticles and Allows Safe Delivery of siRNA and DNA Constructs. *ACS Nano* **2009**, *3*, 3273–3286.
- Astrid, D.; Achim, N. Effects of Particle Size and Molecular Weight of Polyethylenimine on Properties of Nanoparticulate Silicon Dispersions. *J. Am. Ceram. Soc.* **2001**, *84*, 806–812.
- Gottesman, M. M. Mechanisms of Cancer Drug Resistance. *Annu. Rev. Med.* **2002**, *53*, 615–627.
- Szakacs, G.; Paterson, J. K.; Ludwig, J. A.; Booth-Genthe, C.; Gottesman, M. M. Targeting Multidrug Resistance in Cancer. *Nat. Rev. Drug Discovery* **2006**, *5*, 219–234.
- Jabr-Milane, L. S.; van Vlerken, L. E.; Yadav, S.; Amiji, M. M. Multifunctional Nanocarriers to Overcome Tumor Drug Resistance. *Cancer Treat. Rev.* **2008**, *34*, 592–602.
- Ludwig, J. A.; Szakacs, G.; Martin, S. E.; Chu, B. F.; Cardarelli, C.; Sauna, Z. E.; Caplen, N. J.; Fales, H. M.; Ambudkar, S. V.; Weinstein, J. N.; Gottesman, M. M. Selective Toxicity of NSC73306 in MDR1-Positive Cells as a New Strategy to Circumvent Multidrug Resistance in Cancer. *Cancer Res.* **2006**, *66*, 4808–4815.
- Lu, J.; Liong, M.; Zink, J. I.; Tamanoi, F. Mesoporous Silica Nanoparticles as a Delivery System for Hydrophobic Anticancer Drugs. *Small* **2007**, *3*, 1341–1346.
- Ferrari, M. Cancer Nanotechnology: Opportunities and Challenges. *Nat. Rev. Cancer* **2005**, *5*, 161–171.
- Saad, M.; Garbuzenko, O. B.; Minko, T. Co-delivery of siRNA and an Anticancer Drug for Treatment of Multidrug-Resistant Cancer. *Nanomedicine* **2008**, *3*, 761–776.
- Wu, J.; Lu, Y.; Lee, A.; Pan, X. P.; Yang, X.; Zhao, X.; Lee, R. J. Reversal of Multidrug Resistance by Transferrin-Conjugated Liposomes Co-encapsulating Doxorubicin and Verapamil. *J. Pharm. Biopharm. Sci.* **2007**, *10*, 350–357.
- van Vlerken, L. E.; Duan, Z.; Seiden, M. V.; Amiji, M. M. Modulation of Intracellular Ceramide Using Polymeric Nanoparticles to Overcome Multidrug Resistance in Cancer. *Cancer Res.* **2007**, *67*, 4843–4850.
- Chen, A., M.; Zhang, M.; Wei, D.; Stueber, D.; Taratula, O.; Minko, T.; He, H. Co-delivery of Doxorubicin and Bcl-2 siRNA by Mesoporous Silica Nanoparticles Enhances the Efficacy of Chemotherapy in Multidrug-Resistant Cancer Cells. *Small* **2009**, *5*, 2673–2677.

17. Patil, Y. B.; Swaminathan, S. K.; Sadhukha, T.; Ma, L.; Panyam, J. The Use of Nanoparticle-Mediated Targeted Gene Silencing and Drug Delivery to Overcome Tumor Drug Resistance. *Biomaterials* **2009**, *31*, 358–365.
18. Bagwe, R. P.; Hilliard, L. R.; Tan, W. Surface Modification of Silica Nanoparticles to Reduce Aggregation and Nonspecific Binding. *Langmuir* **2006**, *22*, 4357–4362.
19. Santra, S.; Yang, H.; Dutta, D.; Stanley, J. T.; Holloway, P. H.; Tan, W.; Moudgil, B. M.; Mericle, R. A. TAT Conjugated, FITC Doped Silica Nanoparticles for Bioimaging Applications. *Chem. Commun.* **2004**, 2810–2811.
20. Meng, H.; Xia, T.; George, S.; Nel, A. E. A Predictive Toxicological Paradigm for the Safety Assessment of Nanomaterials. *ACS Nano* **2009**, *3*, 1620–1627.
21. Lin, Y.-S.; Haynes, C. L. Synthesis and Characterization of Biocompatible and Size-Tunable Multifunctional Porous Silica Nanoparticles. *Chem. Mater.* **2009**, *21*, 3979–3986.
22. Wang, J.; Huang, M.-h.; Zeng, Z.-x.; Fang, H.-x.; Yang, M.-s. Gene Expression Profiling in Multidrug Resistant KB Cells Using cDNA Microarrays. *Chin. J. Cancer Res.* **2002**, *14*, 5–10.
23. Lim, M. H.; Blanford, C. F.; Stein, A. Synthesis and Characterization of a Reactive Vinyl-Functionalized MCM-41: Probing the Internal Pore Structure by a Bromination Reaction. *J. Am. Chem. Soc.* **1997**, *119*, 4090–4091.